

Band Gaps and Waveguiding in Phoxonic Silicon Crystal Slabs

Y. Pennec,^{1,*} B. Djafari Rouhani,¹ E. H. El Boudouti,^{1,2} C. Li,¹ Y. El Hassouani,¹
J. O. Vasseur,¹ N. Papanikolaou,³ S. Benchabane,⁴ V. Laude,⁴ and A. Martinez⁵

¹*Institut d'Electronique, de Microélectronique et de Nanotechnologie,
UMR CNRS 8520, Université de Lille 1, Villeneuve d'Ascq, France*

²*Laboratoire de Dynamique et d'Optique et des Matériaux, Université d'Oujda, Morocco*

³*Institute of Microelectronics, NCSR, Athena, Greece*

⁴*Institute FEMTO-ST, Université de Franche Comté, ENSMM, Besançon, France*

⁵*Nanophotonics Technology Center, Universidad Politécnica de Valencia, Spain*

(Received April 12, 2010)

We discuss the simultaneous existence of phoxonic, i.e., phononic and photonic, band gaps in a periodic array of holes drilled in a Si membrane. We investigate in detail both the square and the honeycomb lattices. We show that complete phoxonic band gaps can be obtained with the honeycomb lattice. Otherwise, both structures present the possibility of a complete phononic gap together with a photonic band gap of a given symmetry, odd or even, depending on the geometrical parameters. We show the possibility of confinement of both acoustic and optical waves in a waveguide created inside the honeycomb structure.

PACS numbers: 42.70, 42.25.Bs, 42.79.Jq

I. INTRODUCTION

Phononic crystals [1, 2], constituted by a periodical repetition of inclusions in a matrix background have received a great deal of attention during the last two decades [3]. Associated with the possibility of absolute band gaps in their band structure, these materials have found several potential applications, in particular, in the field of wave guiding and filtering [4] (in relation to the properties of their linear and point defects). Recently, the study of phononic crystals slab has become a topic of major interest. Indeed, with an appropriate choice of the geometrical and physical parameters, these finite thickness structures can also exhibit absolute band gaps [5–11]. This makes them suitable for similar applications as in the case of 2D phononic crystals with the additional property of confinement in the vertical direction.

In the photonic crystal counterpart, the medium is made up of periodic dielectric materials and can prohibit the propagation of electromagnetic waves in specific wavelength ranges [12]. Such infinite 2D periodic structures have opened up new features for controlling light, leading to the proposition of many novel devices [13]. Photonic crystal slabs retain, at least approximately, many of the desirable properties of 2D infinite photonic crystals but at the same time are much more easily realized at submicron length scales. Depending on the physical and geometrical parameters, the restriction to finite height of the structure recreates the band gap in the guided modes of the slab below the light cone [14–16].

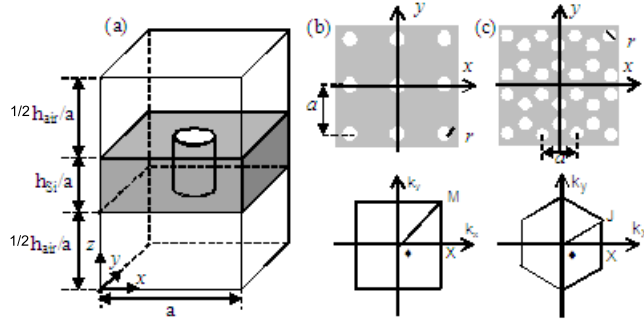


FIG. 1: (a) Representation of the unit cell for the numerical calculations. Square (b) and honeycomb (c) lattices together with the corresponding Brillouin zones. h_{Si} and h_{air} are the thicknesses of the Si slab and air, respectively, in the super-cell considered in the PWE computation. r is the radius of the holes and a the side of the unit cell.

Many studies have investigated separately the existence of photonic and phononic band gaps, but relatively few works have been devoted to simultaneous control of phonons and photons [17–20] and most of the studies are dealing with the case of 2D structures [17–19]. Maldovan and Thomas [17, 18] have shown theoretically that phoxonic band gaps can be obtained in 2D square or hexagonal lattice crystals made up of air holes in a silicon matrix. Sadat-Saleh *et al.* [19] have demonstrated the possibility to open phoxonic band gaps in more complex arrays like multiple cylinders per unit cell in lithium niobate 2D structures. Experimental evidence of such a band gap phenomenon has been reported recently in a 3D phoxonic crystal of amorphous silica spheres [21].

The aim of this paper is to investigate in detail the conditions of existence of simultaneous phononic and photonic band gaps in finite 2D crystals of various structures constituted by a periodic array of holes in a silicon slab. Most of the calculations are performed with the plane-wave expansion (PWE) method, and the convergence of the results is also checked in some cases by using the layered multiple scattering (LMS), finite-difference time domain (FDTD), and finite-element (FE) methods. Section II describes the geometries considered in this paper as well as the method of calculation. Section III presents the results for the most commonly used case of square lattice. Section IV is devoted to the study of the honeycomb lattice. We show in this geometry the existence of a complete photonic and phononic band gap. In the latter structure, we demonstrate in section V the possibility of waveguiding for both optical and acoustic modes. The conclusions are summarized in section VI.

II. GEOMETRY AND METHOD OF CALCULATION

Figure 1 gives the representation of the square and the honeycomb lattices together with the corresponding irreducible Brillouin zone. By considering the lattice period a as the

unit of length, there are several geometrical parameters involved in the problem, namely the thickness h_{Si} of the Si slab, the filling fraction f , and the radius r of the holes. The filling fraction of the air holes in the membrane is given by

$$f = \frac{\pi r^2}{a^2}$$

for the square arrangement and by

$$f = \frac{2\pi r^2}{a^2 \frac{\sqrt{3}}{2}}$$

for the honeycomb structure.

In all the curves presented in the study, the frequencies are given in the dimensionless units $\Omega = \omega a / 2\pi c$, where c is the transverse velocity of sound in silicon for elastic waves and the velocity of light in vacuum for electromagnetic waves.

According to the symmetry of the structure with respect to the middle plane of the slab, the modes can be classified into symmetric (even) and antisymmetric (odd) modes. In a previous work [9], we have demonstrated the existence of absolute phononic band gaps in square and honeycomb lattices of holes in a Si membrane, provided the thickness of the slab is about half of the lattice period and the filling fraction is sufficiently high. In this work, we first concentrate on the existence of a complete phononic band gaps that are calculated for a large variety of the geometrical parameters in the useful ranges (h_{Si}/a from 0.4 to 0.7, and f from 0.3 to 0.7). Then, we search for the photonic band gaps (either complete or for one type of symmetry) in the same ranges of parameters. In general, the complete photonic band gaps (i.e., for both odd and even modes) occur only in a few cases. Otherwise, the phoxonic band gap can be obtained in many situations with a complete phononic gap together with a photonic gap of a given (odd or even) symmetry. Let us mention that in the slab geometry, the photonic gaps have to be searched only below the light cone in vacuum. However, these gaps should preferably occur at dimensionless frequencies Ω below 0.5, otherwise they will be restricted only to a very small area of the Brillouin zone close to the light cone and are therefore not very interesting.

The calculations are generally performed by using the PWE method with periodic conditions applied on each boundary of the super-cell (see Fig. 1(a)). On the phononic side, the air thickness can be reduced to a small slab since elastic waves cannot obviously propagate in vacuum. The air is modeled as a low impedance medium with very low density and very high velocity of sound. The convergence of the calculation is quite fast [9] and it is achieved for a number of plane waves of 1215 for the square lattice and 1815 for the honeycomb structure. Calculations have been checked using two other methods, namely, the finite element (FE) and the finite difference time domain (FDTD). On the photonic side, the thickness of the air slab has been chosen such that it enables the decoupling of the silicon slabs belonging to neighboring super-cells. The air thickness has been chosen equal to $h_{air}/a = 7.4$ to ensure the stability of the whole branches under the light cone, and the calculations have been performed with a number of plane waves equal to 7047. Calculations

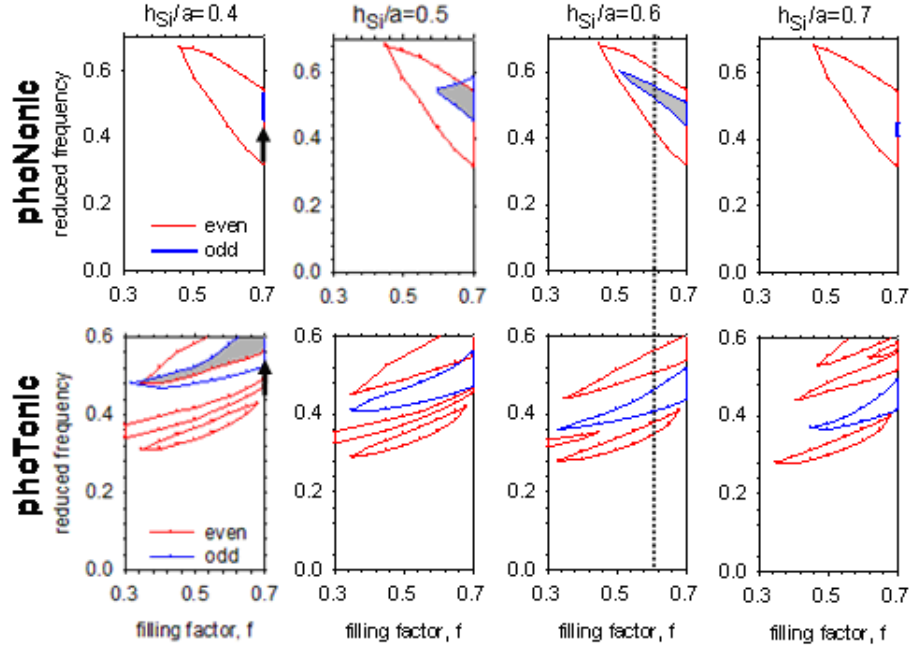


FIG. 2: Simple square lattice: evolution of phononic and photonic gaps of even (red) and odd (blue) symmetries as a function of the filling factor f for different values of the thickness of the silicon slab h_{Si}/a . The grey areas correspond to absolute band gaps.

have been checked using FDTD and the layered multiple scattering (LMS) [22] methods with a good agreement.

III. SQUARE LATTICE

We first present the case of the simple square lattice. Figure 2 reports the evolution of both phononic and photonic gaps for each symmetry, even (red) and odd (blue), as a function of the filling factor f and for a set of silicon plate thicknesses h_{Si}/a in the range $[0.4, 0.7]$.

In this geometry, a complete phoxonic band gap is found only when $h_{Si}/a = 0.4$ and for a high value of the filling factor $f = 0.7$ (black vertical arrow). Unfortunately, from the photonic side, this gap appears in a very restricted region of the Brillouin zone ($\Omega = [0.553, 0.658]$), near the M point, just below the light cone. It means that this solution is not really interesting. To cover the full directions of the Brillouin zone, the reduced frequency value has to be lower than 0.5. Under this condition, there is no overlap between the photonic gaps of both symmetries.

The choice of a phoxonic crystal can be made by searching a structure that exhibits an absolute phononic band gap though a photonic gap of a given symmetry only. Figure

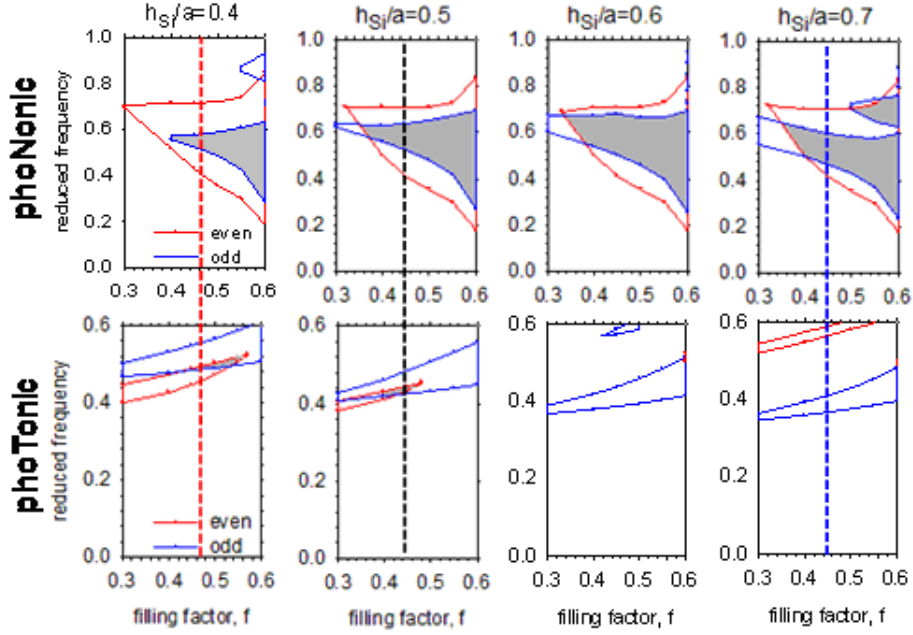


FIG. 3: Honeycomb lattice: evolution in phononic and photonic of the even (red) and odd (blue) gaps as a function of the filling factor f for different values of the thickness of the silicon slab h_{Si}/a . The grey areas correspond to absolute band gaps.

2 shows that in the phononic side, the limitation comes from the odd modes, which only display narrow gaps occurring for a plate thickness of $h_{Si}/a = [0.5, 0.6]$ and for filling factors ($f \geq 0.6$). In this thickness range, there are photonic gaps (either even or odd) at frequencies below 0.5.

For the square lattice structure, one example of phoxonic band gaps for either symmetric (even) or antisymmetric (odd) optical modes can be obtained for the set of parameters ($h_{Si}/a = 0.6$, $f = 0.65$, $r/a = 0.455$) (black vertical dotted line shown in Fig. 2). In view of telecom applications, photonic band gaps have to be chosen close to 1550 nm. Then, the actual geometrical parameters become $a = 701$ nm, $h_{Si} = 421$ nm and $r = 315$ nm for the odd gap and $a = 590$ nm, $h_{Si} = 350$ nm and $r = 265$ nm for the even one, which lead to a mid-gap acoustic frequency of 4.2 GHz and 5.0 GHz respectively. With these parameters, the separation between neighboring holes becomes 70 nm and 60 nm, respectively and makes this phoxonic crystal geometry technologically realizable.

IV. HONEYCOMB LATTICE

Figure 3 represents, for the honeycomb lattice, the evolution of the phononic and photonic band gaps for each symmetry as a function of the filling factor f and for different values of the thickness of the silicon plate h_{Si}/a .

From the phononic side, the honeycomb array is more suitable than the square lattice. Both odd and even gaps are larger and open at lower filling factor. Moreover, one can notice that the absolute phononic band gap exists in the whole investigated range of h_{Si}/a from 0.4 to 0.7. The odd gaps are generally included in the even gaps, except at low filling factor. The limitation comes this time from the photonic side. For the latter, the odd gap exists in the full range of the filling factor and for all values of h_{Si}/a , whereas the even gap is present for $h_{Si}/a \leq 0.5$ and progressively closes when the filling factor increases. Nevertheless, a complete phoxonic band gap, represented by the grey area in Fig. 3, occurs provided the thickness of the slab is in the range $h_{Si}/a = [0.4, 0.5]$. Assuming that the dimensionless photonic frequency gap should be lower than 0.5 to cover the full directions of the Brillouin zone, one can define as an example a set of parameters ($h_{Si}/a = 0.5, f = 0.45, r/a = 0.249$) (black vertical dashed line), which leads to a complete phoxonic band gap. Then, by assuming that the photonic midgap occurs at the telecommunication wavelength of 1550 nm, we find the following geometrical parameters: $a = 687$ nm, $h_{Si} = 330$ nm and the hole radius $r = 171$ nm. The separation between neighboring holes is then 55 nm, which is quite acceptable for the technological fabrication of the sample. With this lattice parameter, the phononic mid-gap frequency occurs at 4.9 GHz.

Although the above example displays simultaneously a complete phononic and photonic band gap, the latter remains relatively narrow. Now, we can discuss more general situations exhibiting a full phononic gap, but a photonic gap of a given symmetry only. One can notice that the photonic band gaps of even symmetry are obtained for the low values of the slab thickness, typically $h_{Si}/a \leq 0.5$, and can be chosen for several filling factors. As an example, the reduced parameters ($h_{Si}/a = 0.4, f = 0.45, r/a = 0.249$) lead to a phoxonic band gap of even photonic symmetry (red vertical dashed line). Phoxonic structures can also be designed with an odd photonic gap, provided the thickness of the slab is $h_{Si}/a \geq 0.5$ in order to ensure that the dimensionless frequency is lower than 0.5. Many filling factors, higher than 0.35, are suitable and one example is given by the following parameters ($h_{Si}/a = 0.7, f = 0.45, r/a = 0.249$) (blue vertical dashed line).

Table I summarizes the main structures suitable to exhibit an absolute phononic band gap together with photonic band gaps either for both or for only one type of symmetry. Of course, the choice of the lengths for the practical realization of the structure depends on the frequency range of interest for specific applications.

V. WAVEGUIDING

Bulk photonic [23] and phononic [24–26] crystals containing rectilinear defects have been shown to guide and control optical and acoustic waves efficiently. Chutinan and Noda [27] have studied linear and bent waveguides in two-dimensional photonic crystal slabs. More recently, Sun and Wu have investigated the propagation of elastic waves through waveguides in a 2D phononic crystal plate made of solid constituents [28]. Vasseur *et al.* [9], using the PWE method, demonstrated the existence of guided modes in an air-silicon phononic crystal plate containing linear defect created inside a square lattice. In

TABLE I: Summary of the most suitable phoxonic crystals and the corresponding band gaps frequencies.

Array	f	r_i/a	h_{Si}/a	PhoNonic band gap	PhoTonic band gap odd modes	PhoTonic band gap even modes	Observations
Square	0.7	0.47	0.4	[0.439, 0.544]		[0.553, 0.658]	-Complete phoxonic gap -Photonic gap at high reduced frequency, in the neighborhood of M -High value of f (holes very close to each other)
Square	0.65	0.45	0.6	[0.472, 0.534]	[0.410, 0.495]	[0.361, 0.400]	-Photonic gap of a given symmetry only
Honeycomb	0.45	0.249	0.48	[0.525, 0.626]		[0.434, 0.454]	-Complete phoxonic gap
Honeycomb	0.45	0.249	0.7	[0.468, 0.611]	[0.368, 0.410]		-Photonic gap of an odd symmetry only
Honeycomb	0.45	0.249	0.4	[0.503, 0.588]		[0.445, 0.492]	-Photonic gap
Honeycomb	0.45	0.249	0.4	[0.503, 0.588]		[0.445, 0.492]	of an even
Honeycomb	0.45	0.249	0.4	[0.503, 0.588]		[0.445, 0.492]	symmetry only

the following, we discuss the conditions of existence of simultaneous phononic and photonic guided modes in finite 2D crystals constituted by a honeycomb array of holes in a silicon slab.

In Fig. 4(a), we consider the periodic crystal constituted of the honeycomb arrangement of air holes in the silicon plate. As seen in section IV, this structure leads to a complete phoxonic band gap when the geometrical parameters are $h_{Si}/a = 0.48$ and $f = 0.45$. One can define a guide by varying the distance between two neighboring rows of holes along the x direction as depicted in Fig. 4(b). The distance d ($d = a/\sqrt{3}$) corresponds to the closest distance between two cylinders in the perfect structure, and α represents the adjustable parameter used for varying the width of the guide, which can be defined by (αd) . Numerically, we consider a rectangular super-cell (Fig. 4(c)) of width a in the x direction. Because of the periodic conditions applied on each boundary of the super-cell, the waveguide is periodically repeated in the y direction. The length L of the super-cell in the y direction has been chosen in such a way to avoid interaction between two neighboring guides. The phononic dispersions curves have been calculated with the help of the finite element method. In

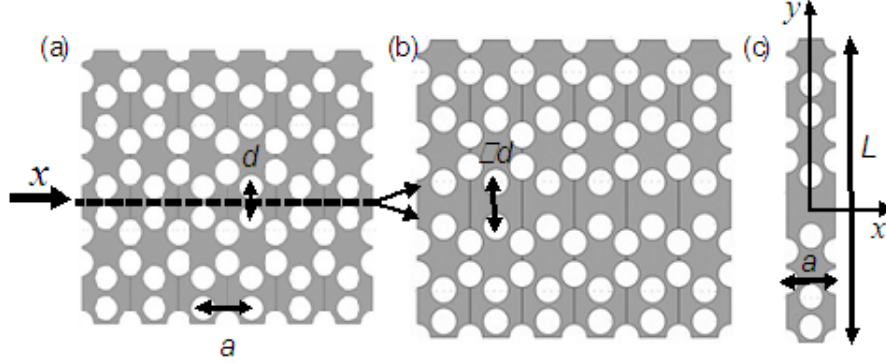


FIG. 4: (a) Honeycomb lattice of air holes drilled in the silicon slab; d is the closest distance between two cylinders. (b) Formation of the waveguide, splitting the structure in the direction x . α represents the factor used for varying the width of the guide. (c) Illustration of the super-cell ($\alpha x L$) in the (x, y) plane used for the FE (phononic) and PWE (photonic) calculations of the band structure of the defected phoxonic crystal plate.

photonic, the band diagrams have been computed with the PWE method and satisfactory convergence has been obtained with a number of reciprocal vectors equal to 3591. The thickness of the super-cell in the z direction remains equal to $(h_{Si} + h_{air})$, as discussed previously in Fig. 1(a).

The evolution of the phononic and photonic (odd and even) dispersion curves of the crystal plate is displayed Fig. 5 for three values of the waveguide widths, namely $\alpha = 1.4, 1.5$ and 1.6 . The dispersion curves are represented in the ΓX direction, corresponding to the direction of propagation of a wave along the linear waveguide. The white areas represent the band gaps delimited by the propagating bands (grey area) of the crystal plate. With the geometrical parameters chosen for the honeycomb lattice, the limits of the absolute band gaps have the following reduced frequencies Ω : $[0.525, 0.626]$ in phononic and $[0.434, 0.454]$ in photonic, as reported Table I.

As a general trend, either in phononic or photonic, the insertion of the waveguide in the perfect structure introduces new modes inside the band gaps of the phoxonic crystal. The number of modes increases with the width of the waveguide. Moreover, these modes shift progressively to the lower frequencies when α increases.

More specifically, in the phononic side, two branches appear in the band gap when $\alpha = 1.4$. The propagation of acoustic waves is monomode in this case. For a wider waveguide with $\alpha = 1.6$ new branches, almost flat, appear at the top of the band gap, and the waveguide becomes multimode at these frequencies. In the photonic side, with $\alpha = 1.4$, one obtains three branches in the odd gap ($[0.434, 0.50]$), whereas no guided modes appear for the even symmetry. By increasing the width of the waveguide to $\alpha = 1.5$ and then to $\alpha = 1.6$, the odd branches shift to lower frequencies, whereas guided modes of even symmetry also appear in the absolute band gap. It is worth noticing that the low group velocities of some of these branches can lead to an enhanced time of interaction between

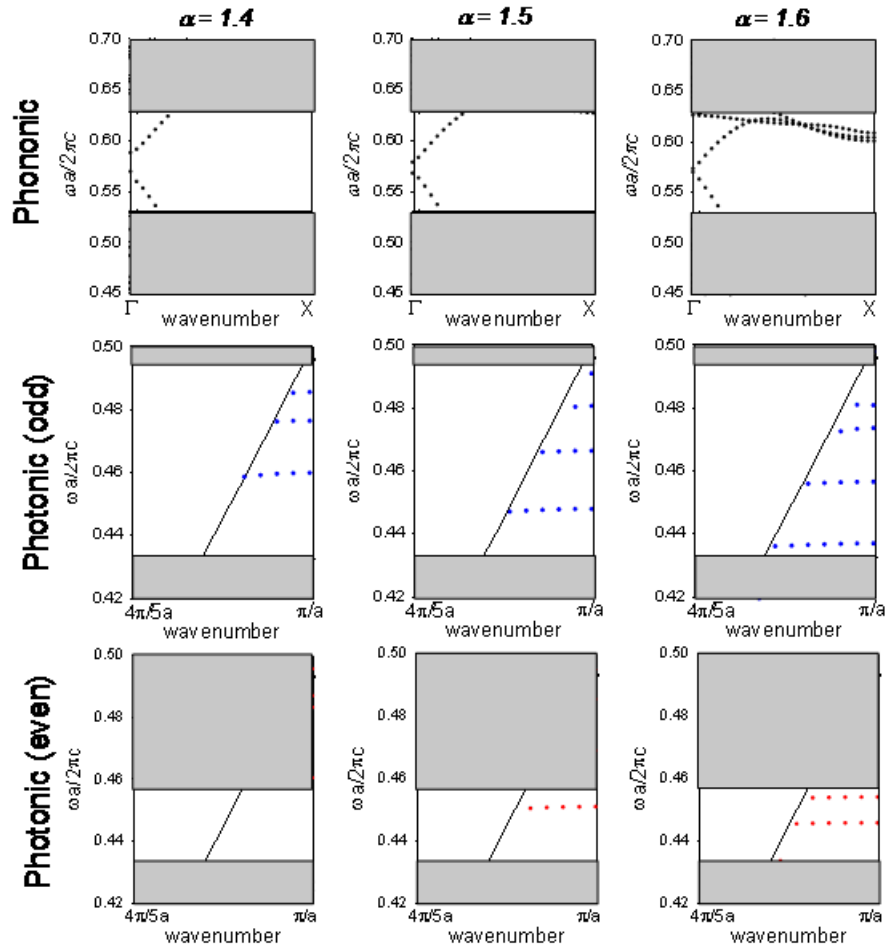


FIG. 5: Band structures along the ΓX direction of the crystal plate containing a waveguide of different widths (αd). For each value of α , the band structures are represented in phononic and photonic (separately for odd and even modes).

the acoustic and optic waves along the waveguide.

With the aim of enhancing phonon-photon interaction, the waveguide width corresponding to $\alpha = 1.6$ emerges as the most suitable case. Indeed, this structure leads to a confinement of the acoustic and optical waves in the same waveguide with slow group velocities that facilitate the interaction between both waves. If the photonic midgap is chosen to be at the telecommunication wavelength, the width of the waveguide becomes $(\alpha d) = 634$ nm.

VI. CONCLUSIONS

We have theoretically investigated the possibilities of opening phoxonics, i.e., phononic and photonic, band gaps in silicon slabs drilled with circular air holes in two different lattices. We have found that the honeycomb lattice presents an absolute phoxonic band gap. Nevertheless, for the square geometry, the simultaneous confinement of both elastic and electromagnetic energy is possible, provided that the optical incident wave is polarized. Finally, we have studied the air silicon phononic crystal plate containing a guide of variable width. We have demonstrated the existence of both acoustic and optical waveguide modes inside the absolute forbidden bands. We have shown that for one value of the width of the guide, low group velocities in both phononic and photonic modes can be obtained. The confinement of both waves in the guide together with their low group velocities should allow the enhancement of photon-phonon interaction. Of course, these results are independent of the scale of the structure. Nevertheless, the parameters have been specified in order to choose the optical wavelengths in the range of telecommunications that leads to acoustic frequencies in the gigahertz regime. Phoxonic crystal slabs hold promises for the simultaneous confinement and tailoring of sound and light waves with potential applications to acousto-optical devices and highly controllable photon-phonon interactions.

Acknowledgments

This work is supported by the European Commission Seventh Framework programs (FP7) under the FET-Open project TAILPHOX N° 233833.

References

- * Electronic address: yan.pennec@univ-lille1.fr
- [1] M. S. Kushwaha, P. Halevi, L. Dobrzynski and B. Djafari-Rouhani, *Phys. Rev. Lett.* **71**, 2022 (1993).
 - [2] M. M. Sigalas and E. N. Economou, *Solid State Commun.* **86**, 141 (1993).
 - [3] For a comprehensive list of references on phononic crystals, see the phononic database at <http://www.phys.uoa.gr/phononics/phononicDatabase.html>
 - [4] Y. Pennec, B. Djafari-Rouhani, J. O. Vasseur, H. Larabi, A. Khelif, A. Choujaa, S. Benchabane, and V. Laude, *Appl. Phys. Lett.* **87**, 261912 (2005).
 - [5] J. C. Hsu and T. T. Wu, *Phys. Rev. B* **74**, 144303 (2006).
 - [6] A. Khelif, B. Aoubiza, S. Mohammadi, A. Adibi, and V. Laude, *Phys. Rev. E* **74**, 046610 (2006).
 - [7] J. O. Vasseur, P. A. Deymier, B. Djafari-Rouhani, and Y. Pennec, *Proc. of IMECE 2006, ASME International Mechanical Engineering Congress and Exhibition, Chicago, Illinois, (5–10, Nov. 2006)*.
 - [8] C. Charles, B. Bonello, and F. Gannot, *Ultrasonics* **44**, 1209(E) (2006).
 - [9] J. O. Vasseur, P. A. Deymier, B. Djafari-Rouhani, Y. Pennec and A. C. Hladky-Hennion, *Phys. Rev. B* **77**, 085415 (2008).

- [10] Y. Pennec, B. Djafari-Rouhani, H. Larabi, J. O. Vasseur and A. C. Hladky-Hennion, *Phys. Rev. B* **78**, 104105 (2008).
- [11] T. T. Wu, Z. G. Huang, T.-C. Tsai, and T. C. Wu, *Appl. Phys. Lett.* **93**, 111902 (2008).
- [12] E. Yablonovitch, *J. Opt. Soc. Am. B* **10**, 283 (1993).
- [13] S. Fan, P. Villeneuve, J. Joannopoulos, and H. Haus, *Optics Express* **3**, 4 (1998).
- [14] S. Shi, C. Chen, and D. W. Prather, *J. Opt. Soc. Am. A* **21**, 1769 (2004).
- [15] S. G. Johnson, S. Fan, P. R. Villeneuve, J. D. Joannopoulos, and L. A. Kolodziejski, *Phys. Rev. B* **60**, 5751 (1999).
- [16] T-I Weng and G. Y. Guo, *J. Appl. Phys.* **99**, 093102 (2006).
- [17] M. Maldovan and E. L. Thomas, *Appl. Phys. Lett.* **88**, 251907 (2006).
- [18] M. Maldovan and E. L. Thomas, *Appl. Phys. B* **83**, 595 (2006).
- [19] S. Sadat-Saleh, S. Benchabane, F. I. Baida, M. P. Bernal and V. Laude, *J. Appl. Phys.* **106**, 074912 (2009).
- [20] Mohammadi S., Eftekhar A. A. and Adibi A., *OSA/CLEO/QELS* (2008).
- [21] A. V. Akimov, Y. Tanaka, A. B. Pevtsov, S. F. Kaplan, V. G. Golubev, S. Tamura, D. R. Yakovlev, and M. Bayer, *Phys. Rev. Lett.* **101**, 033902 (2008).
- [22] I. E. Psarobas, N. Stefanou and A. Modinos, *Phys. Rev. B* **62**, 278 (2000).
- [23] T. F. Krauss, R. M. De La Rue, and S. Brand, *Nature* **383**, 699 (1996).
- [24] M. Torres, F. R. Montero de Espinosa, D. Garcia Pablos, and N. Garcia, *Phys. Rev. Lett.* **82**, 3054 (1999).
- [25] Y. Pennec, B. Djafari-Rouhani, J. O. Vasseur, A. Khelif, and P. A. Deymier, *Phys. Rev. E* **69**, 046608 (2004).
- [26] A. Khelif, A. Choujaa, S. Benchabane, B. Djafari-Rouhani, and V. Laude, *Z. Kristallogr.* **220**, 836 (2005).
- [27] Chutinan and Noda, *Phys. Rev. B* **62**, 4488 (2000).
- [28] J.-H. Sun and T. T. Wu, *Phys. Rev. B* **76**, 104304 (2007).